NSLS-II FAST ORBIT FEEDBACK SYSTEM *

Y. Tian#, K. Ha, L. Yu, W. Cheng, J. DeLong, L. Dalesio, BNL, Upton, NY 11973, USA
W. Levine, University of Maryland, College Park, MD 20742, USA

Abstract

This paper presents the NSLS-II fast orbit feedback (FOFB) system, including the architecture, the algorithm and the commissioning results. A two-tier communication architecture is used to distribute the 10kHz beam position data (BPM) around the storage ring. The FOFB calculation is carried out in field programmable gate arrays (FPGA). An individual eigenmode compensation algorithm is applied to allow different eigenmodes to have different compensation parameters. The system is used as a regular tool to maintain the beam stability at NSLS-II.

INTRODUCTION

NSLS-II is a third generation 3GeV storage ring with ultra-low emittance [1]. The low emittance requires a very stable electron beam orbit. Applying the common rule (beam stability < 10% of beam size), NSLS-II needs to hold submicron beam orbit stability. The stringent orbit stability requires the orbit feedback system to be able to suppress various noises from low frequency ground motion to high frequency mechanical vibration [2].

The NSLS2 BPM electronics generates high resolution turn-by-turn, fast acquisition (10kHz) and slow acquisition (10Hz) data. Fast acquisition data is used for global fast orbit feedback. To ensure sufficient bandwidth of the feedback loop, 10kHz data from all storage ring BPMs are distributed within a short period of time. A two-tier communication architecture is implemented to ensure the time budget for the FOFB system is satisfied. The first tier is the communication between local BPMs and the cell controller at each cell. The second tier is the communication between the cells around the whole storage ring.

The FOFB system is a typical multiple-input and multiple-output (MIMO) system. One common feature of the traditional singular value decomposition (SVD) based orbit feedback algorithm is that it applies the same controller dynamics (such as a PID controller) to all eigenmodes. Since each eigenmode has a different frequency response, it is desirable to apply a different controller for each of the eigenmodes and thus each eigenmode has different compensation in the frequency domain [3]. The challenge for such individual eigenmode compensation is that the feedback system needs to carry out much larger calculations within the time budget of the FOFB system. In this paper, we present the implementation and commissioning results of the FOFB system at NSLS-II.

*Work supported by DOE contract No: DE-AC02-98CH10886
#ytian@bnl.gov

TWO-TIER COMMUNICATION

One common task for a global orbit feedback system is to deliver BPM data to the calculation unit, and to send the calculated result, i.e. the corrector setpoints, to the power supplies. Many communication protocols are used in different labs.

To design the communication protocol at NSLS-II, we take advantage of the geographic locations of BPMs and correctors at NSLS-II. The NSLS-II storage ring is separated into 30 cells. There are 6 BPMs, 3 fast correctors, and 6 slow correctors in each cell. To effectively deliver the BPM and corrector data, we designed a hardware unit in each cell to collect local BPM data, deliver the BPM data around the ring, and to send corrector setpoints to the correctors. We call this unit the cell controller.

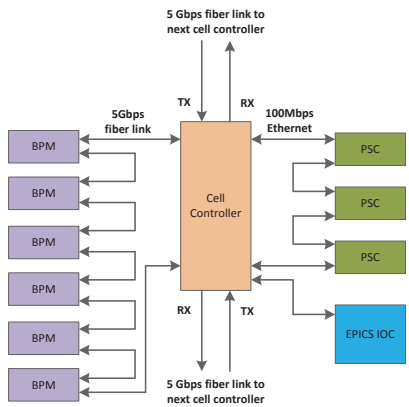

Figure 1: Two-tier communication.

By using cell controllers, two-tier communication is established, as shown in Figure 1. The first tier is the communication of the local data in one cell. In one cell, the cell controller and up to 12 BPMs are connected using fiber optic cables to form a ring structure. Currently, FOFB is only using 6 RF BPMs in the loop and it can be expanded to include 6 ID BPMs or X-ray BPMs. Each BPM sends its position data to its left and right neighbours, and passes through its neighbours' data. The data finally reach the cell controller and the cell controller saves the 6 local BPMs' data in its buffer. This communication protocol is called a serial device interface (SDI). On the other side, the corrector setpoints are sent from the cell controller to the local fast correctors via a similar SDI link. The only difference is that the power supply SDI link uses Ethernet PHY.

The second-tier communication is between the 30 cell controllers. The 30 cell controllers are connected using fiber optic cable to form a ring structure. Each cell

ISBN 978-3-95450-148-9

controller sends the local BPM data to its neighbour cell. Within 14us, each cell controller has all the BPM data. It is worth mentioning that the SDI protocol includes a clockwise and counter clockwise ring structure. The data communication has built-in redundancy.

COMPENSATION IN EIGENSPACE

The NSLS-II FOFB system applies a novel approach of feedback compensation in eigenspace [4]. Figure 2 shows the diagram of eigenspace decoupling and compensation in each eigenmode.

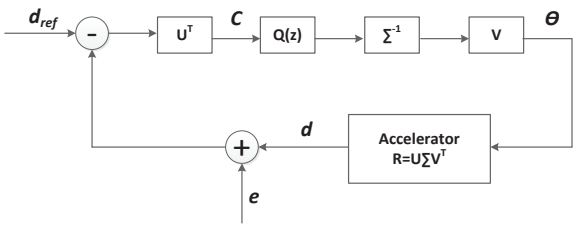

Figure 2: FOFB with eigenspace compensation.

In Figure 2, $\vec{e}$ is used to represent the noise in the system and $\vec{c}$ is used to represent the eigenspace projection of each input

$$\vec{c} = U^T(\vec{d} - \vec{d}_{ref} + \vec{e})$$

For each of the components of $\vec{c}$, an individual digital controller can be designed for the compensation of each eigenmode. The MIMO problem is converted to many signal-input signal-output (SISO) problems, for which control theory has many standard solutions. We use $Q_i(z)$ to represent the digital controller applied only on *ith* eigencomponent of $\vec{c}$.

The above eigenspace compensation algorithm allows us to apply different compensation parameters (for example, PID values) to each eigenmode and thus provide a flexible controller according to each eigenspace's transfer function. On the other hand, such an algorithm needs much many calculations than the traditional algorithm.

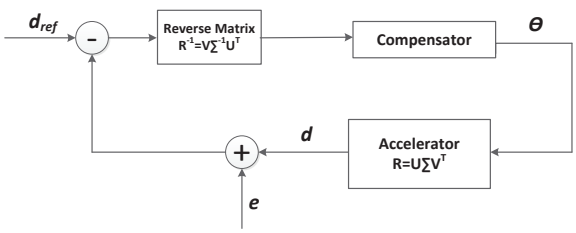

Figure 3: A typical SVD-based FOFB system.

Figure 3 shows a typical SVD-based FOFB algorithm. It shows that to calculate one corrector setpoint, the system needs to multiply one row of the reverse response matrix by the orbit error. This needs M multiply–accumulate (MAC) operations, where M is the number of BPMs. A typical PID compensator adds another 3 MACs. The total calculation amount is M+3 MACs.

For eigenspace compensation, as shown in Figure 2, the orbit error needs to first multiply each row of the U^T matrix to decouple into eigen components in eigenspace. Then a compensator is applied for each eigenmode. The third step is to combine all eigen components into corrector space by multiplying the eigen components by the V matrix. Apparently, due to the eigenspace decoupling, the amount of calculation increases by N times, where N is the number of eigenmodes. For NSLS-II, N is 180. Such a large number of calculation needs to be finished within the 100us FOFB timing budget. This is a challenge for NSLS-II FOFB system.

We solved the challenge by using hardware for the FOFB calculation. Instead of using a general CPU to do the eigenspace compensation, we used FPGAs for the calculation. Figure 4 shows that most of the calculation is in the decoupling process, where each row of the U^T matrix multiplies the orbit difference. We noticed that this process can be done in parallel. Compared to serial computing using a CPU, FPGAs are well known for their parallel computation capability.

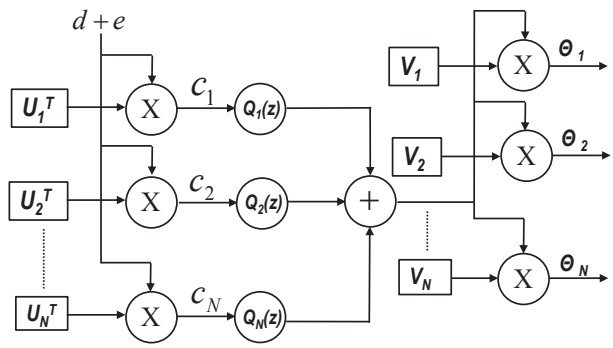

Figure 4: FOFB calculations with FPGA.

Figure 4 shows the basic calculation unit of FOFB inside FPGA. It includes the parallel decoupling in eigenspace together with the corrector setpoint calculation in parallel. Floating point calculation is used to make the calculation more accurate.

COMMISSIOING RESULTS

The NSLS-II FOFB system was commissioned and proved to meet the requirements of the orbit stability. Since June 2015, the FOFB system has been a regular tool to maintain beam stability.

Beam Stability Requirement

There are 30 double-bend achromat (DBA) cells in NSLS-II storage ring. The insertion devices are located at the straight sections of 15 high beta (long) and low beta (short) sections. Three damping wigglers are installed to reduce the bare lattice horizontal emittance from 2nm.rad

ISBN 978-3-95450-148-9

to 0.9nm.rad. Figure 5 shows the RMS beam size in one super cell.

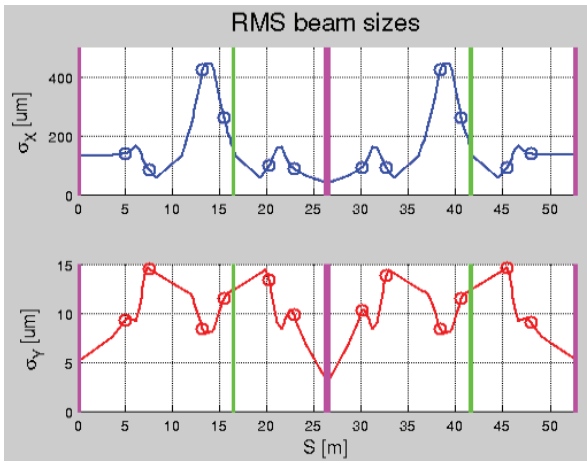

Figure 5: RMS beam size in one supercell using emittance of $\varepsilon_x/\varepsilon_y$ = 0.9/0.008 nm.rad and energy spread of 0.09%.

The photon beamline source points are marked with green and pink vertical lines. The beam stability requirement for FOFB is that the beam movement is less than 10% of beam size. One can see that the most stringent requirement is to keep beam motion less than 300nm at s value about 27m, where the RMS beam size is 3us.

Beam Stability Achievement

Figures 6 and 7 show the beam stability with FOFB on and off. Figure 6 is the power spectrum density (PSD) plot for FOFB on and off cases. The power spectrum of each BPM is calculated from 10 second synchronized 10kHz fast acquisition data. Different BPMs at different locations have different spectra. Figure 6 shows the average spectrum for all non-dispersion BPMs. There are three panes in Figure 6: the upper one shows the spectrum for the horizontal and vertical planes, the middle one shows the integrated spectrum where the integration starts from low frequency and the lower pane shows the integrated spectrum where the integration starts from high frequency. Figure 6 shows that the FOFB system is able to supress noises up to 250Hz in the vertical plane and up to 50Hz in horizontal plane. During the commissioning, most of the effort was spent on vertical plane noise suppression. Feedback parameters can be further optimized in the future developments.

Figure 7 shows the RMS motion of 12 BPMs in one supercell (C02-C03) for both the horizontal and vertical planes. The data is calculated from the integration of PSD from 1 Hz to 500Hz. The dashed lines are drawn to indicate 1% of horizontal beam size and 10% of vertical beam size. In the horizontal plane, the RMS motion is suppressed within 1% of beam size when FOFB is on. This is well within the requirement. In the vertical plane, when FOFB is off, the beam motion is about 20% of beam size. With FOFB on, the beam motion is suppressed down to about 5% of beam motion, which is also within the 10% of requirement. The HXN (Hard X-ray Nano Probe) beamline has the most stringent requirement for orbit stability. C03 IVU, which locates in the middle waist, is the insertion device for the HXN beamline. From the two BPM readings at the two ends of the insertion device, position and angle spectrum at the IVU center can be calculated. In the vertical plane, the integrated (from 1Hz to 500Hz) position and angle motions are 0.216 μm and 0.136 μrad, within the 10% beam size and 10% of beam angle divergence requirement.

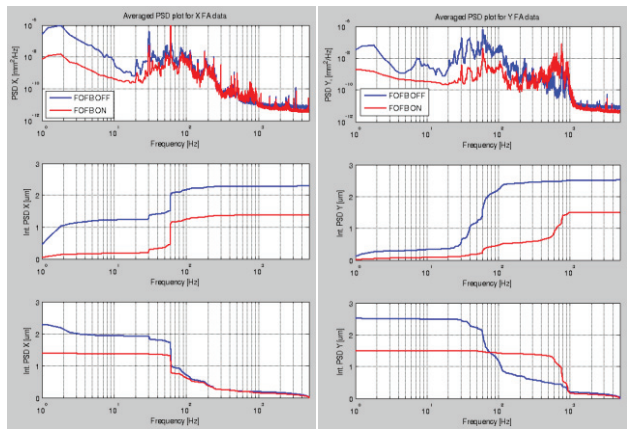

Figure 6: BPM 10kHz FA data PSD spectrum.

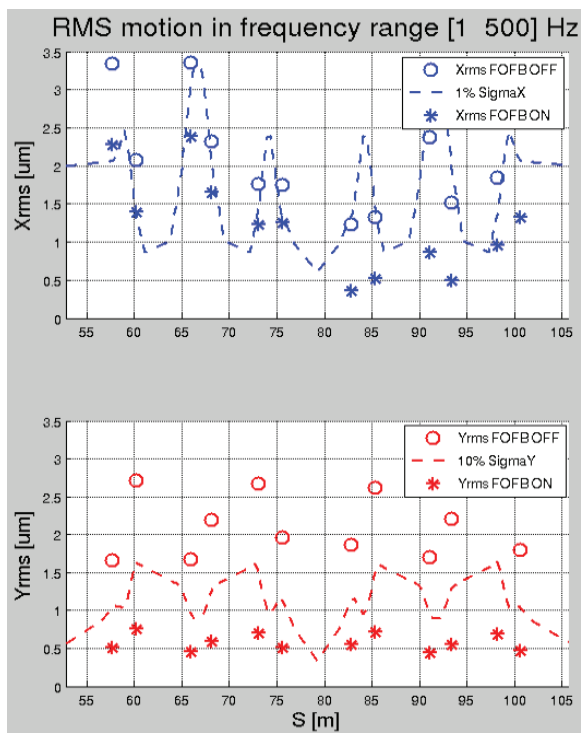

Figure 7: Integrated RMS motion(1-500Hz) for 12 BPMs in one supercell (C02-C03).

ISBN 978-3-95450-148-9

DISCUSSIONS

FOFB on During Injection

Before the top-off operation, NSLS-II had been operated with regular injection. Usually the beam was injected when the stored beam density drops to some level. During our beam study, we found that the beam orbit change during beam injection was small. This is due to the relatively small injection beam charge and the matched optics design between the storage beam and injection beam. The small disturbance allowed FOFB to stay on during injection.

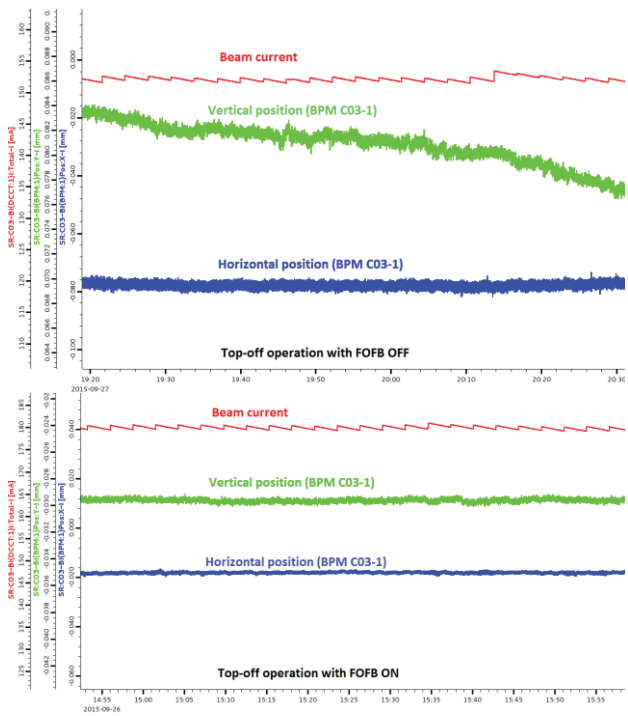

Figure 8: BPM position (10Hz data) during top-off operation with FOFB off (top) and FOFB on (bottom)

NSLS-II top-off operation was commissioned in September 2015. Figure 8 shows the BPM 10Hz reading during top-off operation with FOFB off and FOFB on. It shows the noise suppression effect of FOFB system. With FOFB on, the horizontal and vertical orbit disturbance during beam injection is negligible. Starting from October 1, 2015, NSLS-II is running with both FOFB on and top-off mode to provide users a stable beam current and stable beam orbit.

FOFB on with Insertion Device(ID) Cap change

Light source users regularly change the insertion gaps. The change brings some orbit disturbance. To keep the orbit disturbance small, lookup tables are carefully designed to compensate the disturbance caused by ID gap changes.

During commissioning, we verified that if ID lookup tables are designed well, the leaking orbit disturbance is small and the FOFB can compensate such disturbances. One exception is the damping wiggler. The movement of the damping wiggler causes large orbit change and FOFB can't easily compensate it. Fortunately, the change of damping wiggler doesn't happen often. The FOFB can be turned off before the movement, and turned on after the damping wiggler movement.

FOFB with Local Bump Creation

During the NSLS-II beam line commissioning stage, beam line users are allowed to create a local bump for a specific angle and offset at ID center. A high level application has been designed to create such local bump using multiple local slow correctors. If FOFB stays on during local bump creation, the two systems fight with each other: FOFB is trying to keep the orbit to its own reference orbit and the local bump program is trying to create a new orbit. We have tested several methods to solve this problem. The principle is to quickly change the reference orbit of the FOFB system. We are in the process of testing different methods to change the FOFB reference orbit.

SUMMARY

This paper discussed the architecture, the calculation algorithm and the commissioning results of the NSLS-II FOFB system. It shows some of the novel approaches of the fast orbit feedback system: two tier communication protocol, eigenspace compensation, and FOFB calculation using FPGA. These novel approaches provide flexibility for FOFB control and they demonstrate the performance required to meet all NSLS-II sub-micron beam stability design goals with noise suppression up to 250Hz in the vertical plane. The FOFB system is commissioned and used as a regular tool for user operation. We also discussed various issues during FOFB commissioning.

ACKNOWLEDGEMENTS

Many critical subsystems are required to work well to make the FOFB system work. We thank O. Singh, K. Vetter, J. Mead, A. Dellapenna and Y. Hu for their efforts of BPM development. We also thank G. Ganetis, W. Louie and J. Ricciardelli for fast corrector power development.

REFERENCES

[1] S. Ozaki, et.al, "Philosophy for NSLS-II Design with Sub-nanometer Horizontal Emittance", Proceedings PAC07, p.77 (2007).

[2] L. Yu, "Performance Calculation on Orbit Feedback for NSLS-II", Proceedings PAC05, p.1036 (2005).

[3] M.G.Abbott, et.al, "Performance and Future Development of the Diamond Fast Orbit Feedback System", Proceedings of EPAC08, p.3257 (2008).

[4] Y. Tian, et.al, "NSLS-II Fast Orbit Feedback with Individual Eigenmode Compensation", Proceedings PAC11, p.1488 (2011).

ISBN 978-3-95450-148-9